

Measurement of the isolated photon cross section in $p\bar{p}$ collisions at $\sqrt{s} = 1.96$ TeV

DØ Collaboration

V.M. Abazov^{aj}, B. Abbott^{bw}, M. Abolins^{bm}, B.S. Acharya^{ac}, M. Adams^{az}, T. Adams^{ax}, M. Agelou^r, J.-L. Agram^s, S.H. Ahn^{ae}, M. Ahsan^{bg}, G.D. Alexeev^{aj}, G. Alkhazov^{an}, A. Alton^{bl}, G. Alverson^{bk}, G.A. Alves^b, M. Anastasoae^{ai}, T. Andeen^{bb}, S. Anderson^{at}, B. Andrieu^q, Y. Arnaudⁿ, M. Arov^{ba}, A. Askew^{ax}, B. Åsman^{ao}, A.C.S. Assis Jesus^c, O. Atramentov^{be}, C. Autermann^u, C. Avila^h, F. Badaud^m, A. Baden^{bi}, L. Bagby^{ba}, B. Baldin^{ay}, P.W. Balm^{ah}, D.V. Bandurin^{aj,*}, P. Banerjee^{ac}, S. Banerjee^{ac}, E. Barberis^{bk}, P. Bargassa^{cb}, P. Baringer^{bf}, C. Barnes^{ar}, J. Barreto^b, J.F. Bartlett^{ay}, U. Bassler^q, D. Bauer^{bc}, A. Bean^{bf}, S. Beauceron^q, M. Begalli^c, M. Begel^{bs}, A. Bellavance^{bo}, S.B. Beri^{aa}, G. Bernardi^q, R. Bernhard^{ap}, L. Berntzon^o, I. Bertram^{aq}, M. Besançon^r, R. Beuselinck^{ar}, V.A. Bezzubov^{am}, P.C. Bhat^{ay}, V. Bhatnagar^{aa}, M. Binder^y, C. Biscarat^{aq}, K.M. Black^{bj}, I. Blackler^{ar}, G. Blazey^{ba}, F. Blekman^{ar}, S. Blessing^{ax}, D. Bloch^s, U. Blumenschein^w, A. Boehnlein^{ay}, O. Boeriu^{bd}, T.A. Bolton^{bg}, F. Borchering^{ay}, G. Borissov^{aq}, K. Bos^{ah}, T. Bose^{br}, A. Brandt^{bz}, R. Brock^{bm}, G. Brooijmans^{br}, A. Bross^{ay}, D. Brown^{bz}, N.J. Buchanan^{ax}, D. Buchholz^{bb}, M. Buehler^{cc}, V. Buescher^w, S. Burdin^{ay}, S. Burke^{at}, T.H. Burnett^{cd}, E. Busato^q, C.P. Buszello^{ar}, J.M. Butler^{bj}, S. Calvet^o, J. Cammin^{bs}, S. Caron^{ah}, W. Carvalho^c, B.C.K. Casey^{by}, N.M. Cason^{bd}, H. Castilla-Valdez^{ag}, S. Chakrabarti^{ac}, D. Chakraborty^{ba}, K.M. Chan^{bs}, A. Chandra^{ac}, D. Chapin^{by}, F. Charles^s, E. Cheu^{at}, D.K. Cho^{bj}, S. Choi^{af}, B. Choudhary^{ab}, T. Christiansen^y, L. Christofek^{bf}, D. Claes^{bo}, B. Clément^s, C. Clément^{ao}, Y. Coadou^e, M. Cooke^{cb}, W.E. Cooper^{ay}, D. Coppage^{bf}, M. Corcoran^{cb}, M.-C. Cousinou^o, B. Cox^{as}, S. Crépe-Renaudinⁿ, D. Cutts^{by}, H. da Motta^b, A. Das^{bj}, M. Das^{bh}, B. Davies^{aq}, G. Davies^{ar}, G.A. Davis^{bb}, K. De^{bz}, P. de Jong^{ah}, S.J. de Jong^{ai}, E. De La Cruz-Burelo^{bl}, C. De Oliveira Martins^c, S. Dean^{as}, J.D. Degenhardt^{bl}, F. Déliot^r, M. Demarteau^{ay}, R. Demina^{bs}, P. Demine^r, D. Denisov^{ay}, S.P. Denisov^{am}, S. Desai^{bt}, H.T. Diehl^{ay}, M. Diesburg^{ay}, M. Doidge^{aq}, H. Dong^{bt}, S. Doulas^{bk}, L.V. Dudko^{al}, L. Duflot^p, S.R. Dugad^{ac}, A. Duperrin^o, J. Dyer^{bm}, A. Dyshkant^{ba}, M. Eads^{bo}, D. Edmunds^{bm}, T. Edwards^{as}, J. Ellison^{aw}, J. Elmsheuser^y, V.D. Elvira^{ay}, S. Eno^{bi}, P. Ermolov^{al}, J. Estrada^{ay}, H. Evans^{bc}, A. Evdokimov^{ak}, V.N. Evdokimov^{am}, J. Fast^{ay}, S.N. Fatakia^{bj}, L. Feligioni^{bj}, A.V. Ferapontov^{am}, T. Ferbel^{bs}, F. Fiedler^y, F. Filthaut^{ai}, W. Fisher^{ay}, H.E. Fisk^{ay}, I. Fleck^w, M. Fortner^{ba}, H. Fox^w, S. Fu^{ay}, S. Fuess^{ay}, T. Gadfort^{cd}, C.F. Galea^{ai}, E. Gallas^{ay}, E. Galyaev^{bd}, C. Garcia^{bs}, A. Garcia-Bellido^{cd}, J. Gardner^{bf}, V. Gavrilov^{ak}, A. Gay^s, P. Gay^m, D. Gelé^s, R. Gelhaus^{aw}, C.E. Gerber^{az}, Y. Gershtein^{ax}, D. Gillberg^e, G. Ginther^{bs}, T. Golling^v, N. Gollub^{ao}, B. Gómez^h, K. Gounder^{ay}, A. Goussiou^{bd}, P.D. Grannis^{bt}, S. Greder^c, H. Greenlee^{ay}, Z.D. Greenwood^{bh}, E.M. Gregores^d, G. Grenier^t, Ph. Gris^m, J.-F. Grivaz^p, S. Grünendahl^{ay}, M.W. Grünwald^{ad}, G. Gutierrez^{ay}, P. Gutierrez^{bw}, A. Haas^{br}, N.J. Hadley^{bi}, S. Hagopian^{ax}, J. Haley^{bp}, I. Hall^{bw}, R.E. Hall^{av}, C. Han^{bl},

L. Han^g, K. Hanagaki^{ay}, K. Harder^{bg}, A. Harel^z, R. Harrington^{bk}, J.M. Hauptman^{be}, R. Hauser^{bm},
 J. Hays^{bb}, T. Hebbeker^u, D. Hedin^{ba}, J.G. Hegeman^{ah}, J.M. Heinmiller^{az}, A.P. Heinson^{aw},
 U. Heintz^{bj}, C. Hensel^{bf}, G. Hesketh^{bk}, M.D. Hildreth^{bd}, R. Hirosky^{cc}, J.D. Hobbs^{bt},
 B. Hoeneisen^l, M. Hohlfeld^p, S.J. Hong^{ae}, R. Hooper^{by}, P. Houben^{ah}, Y. Hu^{bt}, J. Huang^{bc},
 V. Hynekⁱ, I. Iashvili^{bq}, R. Illingworth^{ay}, A.S. Ito^{ay}, S. Jabeen^{bf}, M. Jaffré^p, S. Jain^{bw}, V. Jain^{bu},
 K. Jakobs^w, C. Jarvis^{bi}, A. Jenkins^{ar}, R. Jesik^{ar}, K. Johns^{at}, C. Johnson^{br}, M. Johnson^{ay},
 A. Jonckheere^{ay}, P. Jonsson^{ar}, A. Juste^{ay}, D. Käfer^u, S. Kahn^{bu}, E. Kajfasz^o, A.M. Kalinin^{aj},
 J.M. Kalk^{bh}, J.R. Kalk^{bm}, D. Karmanov^{al}, J. Kasper^{bj}, I. Katsanos^{br}, D. Kau^{ax}, R. Kaur^{aa},
 R. Kehoe^{ca}, S. Kermiche^o, S. Kesisoglou^{by}, A. Khanov^{bx}, A. Kharchilava^{bq}, Y.M. Kharzheev^{aj},
 D. Khatidze^{br}, H. Kim^{bz}, T.J. Kim^{ae}, B. Klima^{ay}, J.M. Kohli^{aa}, J.-P. Konrath^w, M. Kopal^{bw},
 V.M. Korablev^{am}, J. Kotcher^{bu}, B. Kothari^{br}, A. Koubarovsky^{al}, A.V. Kozelov^{am}, J. Kozminski^{bm},
 A. Kryemadhi^{cc}, S. Krzywdzinski^{ay}, A. Kumar^{bq}, S. Kunori^{bi}, A. Kupco^k, T. Kurča^t, J. Kvitaⁱ,
 S. Lager^{ao}, S. Lammers^{br}, G. Landsberg^{by}, J. Lazoflores^{ax}, A.-C. Le Bihan^s, P. Lebrun^t,
 W.M. Lee^{ax}, A. Leflat^{al}, F. Lehner^{ap}, C. Leonidopoulos^{br}, V. Lesne^m, J. Leveque^{at}, P. Lewis^{ar},
 J. Li^{bz}, Q.Z. Li^{ay}, J.G.R. Lima^{ba}, D. Lincoln^{ay}, S.L. Linn^{ax}, J. Linnemann^{bm}, V.V. Lipaev^{am},
 R. Lipton^{ay}, L. Lobo^{ar}, A. Lobodenko^{an}, M. Lokajicek^k, A. Lounis^s, P. Love^{aq}, H.J. Lubatti^{cd},
 L. Lueking^{ay}, M. Lynker^{bd}, A.L. Lyon^{ay}, A.K.A. Maciel^b, R.J. Madaras^{au}, P. Mättig^z, C. Magass^u,
 A. Magerkurth^{bl}, A.-M. Magnanⁿ, N. Makovec^p, P.K. Mal^{bd}, H.B. Malbouisson^c, S. Malik^{bo},
 V.L. Malyshev^{aj}, H.S. Mao^f, Y. Maravin^{bg}, M. Martens^{ay}, S.E.K. Mattingly^{by}, R. McCarthy^{bt},
 R. McCroskey^{at}, D. Meder^x, A. Melnitchouk^{bn}, A. Mendes^o, L. Mendoza^h, M. Merkin^{al},
 K.W. Merritt^{ay}, A. Meyer^u, J. Meyer^v, M. Michaut^r, H. Miettinen^{cb}, J. Mitrevski^{br}, J. Molina^c,
 N.K. Mondal^{ac}, J. Monk^{as}, R.W. Moore^e, T. Moulik^{bf}, G.S. Muanza^t, M. Mulders^{ay}, L. Mundim^c,
 Y.D. Mutaf^{bt}, E. Nagy^o, M. Naimuddin^{ab}, M. Narain^{bj}, N.A. Naumann^{ai}, H.A. Neal^{bl}, J.P. Negret^h,
 S. Nelson^{ax}, P. Neustroev^{an}, C. Noeding^w, A. Nomerotski^{ay}, S.F. Novaes^d, T. Nunnemann^y,
 E. Nurse^{as}, V. O'Dell^{ay}, D.C. O'Neil^e, G. Obrant^{an}, V. Oguri^c, N. Oliveira^c, N. Oshima^{ay},
 G.J. Otero y Garzón^{az}, P. Padley^{cb}, N. Parashar^{ay,l}, S.K. Park^{ae}, J. Parsons^{br}, R. Partridge^{by},
 N. Parua^{bt}, A. Patwa^{bu}, G. Pawloski^{cb}, P.M. Perea^{aw}, E. Perez^r, P. Pétroff^p, M. Petteni^{ar},
 R. Piegaia^a, M.-A. Pleier^v, P.L.M. Podesta-Lerma^{ag}, V.M. Podstavkov^{ay}, Y. Pogorelov^{bd},
 M.-E. Pol^b, A. Pompoš^{bw}, B.G. Pope^{bm}, W.L. Prado da Silva^c, H.B. Prosper^{ax}, S. Protopopescu^{bu},
 J. Qian^{bl}, A. Quadt^v, B. Quinn^{bn}, K.J. Rani^{ac}, K. Ranjan^{ab}, P.A. Rapidis^{ay}, P.N. Ratoff^{aq},
 S. Reucroft^{bk}, M. Rijssenbeek^{bt}, I. Ripp-Baudot^s, F. Rizatdinova^{bx}, S. Robinson^{ar}, R.F. Rodrigues^c,
 C. Royon^r, P. Rubinov^{ay}, R. Ruchti^{bd}, V.I. Rud^{al}, G. Sajotⁿ, A. Sánchez-Hernández^{ag},
 M.P. Sanders^{bi}, A. Santoro^c, G. Savage^{ay}, L. Sawyer^{bh}, T. Scanlon^{ar}, D. Schaile^y,
 R.D. Schamberger^{bt}, Y. Scheglov^{an}, H. Schellman^{bb}, P. Schieferdecker^y, C. Schmitt^z,
 C. Schwanenberger^v, A. Schwartzman^{bp}, R. Schwienhorst^{bm}, S. Sengupta^{ax}, H. Severini^{bw},
 E. Shabalina^{az}, M. Shamim^{bg}, V. Shary^r, A.A. Shchukin^{am}, W.D. Shephard^{bd}, R.K. Shivpuri^{ab},
 D. Shpakov^{bk}, R.A. Sidwell^{bg}, V. Simak^j, V. Sirotenko^{ay}, P. Skubic^{bw}, P. Slattery^{bs}, R.P. Smith^{ay},
 K. Smolek^j, G.R. Snow^{bo}, J. Snow^{bv}, S. Snyder^{bu}, S. Söldner-Rembold^{as}, X. Song^{ba},
 L. Sonnenschein^q, A. Sopczak^{aq}, M. Sosebee^{bz}, K. Soustruznikⁱ, M. Souza^b, B. Spurlock^{bz},
 J. Starkⁿ, J. Steele^{bh}, K. Stevenson^{bc}, V. Stolin^{ak}, A. Stone^{az}, D.A. Stoyanova^{am}, J. Strandberg^{ao},
 M.A. Strang^{bq}, M. Strauss^{bw}, R. Ströhmer^y, D. Strom^{bb}, M. Strovink^{au}, L. Stutte^{ay},
 S. Sumowidagdo^{ax}, A. Sznajder^c, M. Talby^o, P. Tamburello^{at}, W. Taylor^e, P. Telford^{as}, J. Temple^{at},
 B. Tiller^y, M. Titov^w, M. Tomoto^{ay}, T. Toole^{bi}, I. Torchiani^w, S. Towers^{aq}, T. Trefzger^x,
 S. Trincaz-Duvoid^q, D. Tsybychev^{bt}, B. Tuchming^r, C. Tully^{bp}, A.S. Turcot^{as}, P.M. Tuts^{br},
 L. Uvarov^{an}, S. Uvarov^{an}, S. Uzunyan^{ba}, B. Vachon^e, P.J. van den Berg^{ah}, R. Van Kooten^{bc},

W.M. van Leeuwen^{ah}, N. Varelas^{az}, E.W. Varnes^{at}, A. Vartapetian^{bz}, I.A. Vasilyev^{am}, M. Vaupel^z,
 P. Verdier^t, L.S. Vertogradov^{aj}, M. Verzocchi^{ay}, F. Villeneuve-Segulier^{ar}, J.-R. Vlimant^q,
 E. Von Toerne^{bg}, M. Voutilainen^{bo,2}, M. Vreeswijk^{ah}, T. Vu Anh^p, H.D. Wahl^{ax}, L. Wang^{bi},
 J. Warchol^{bd}, G. Watts^{cd}, M. Wayne^{bd}, M. Weber^{ay}, H. Weerts^{bm}, N. Vermes^v, M. Wetstein^{bi},
 A. White^{bz}, V. White^{ay}, D. Wicke^{ay}, D.A. Wijngaarden^{ai}, G.W. Wilson^{bf}, S.J. Wimpenny^{aw},
 M. Wobisch^{ay}, J. Womersley^{ay}, D.R. Wood^{bk}, T.R. Wyatt^{as}, Y. Xie^{by}, Q. Xu^{bl}, N. Xuan^{bd},
 S. Yacoob^{bb}, R. Yamada^{ay}, M. Yan^{bi}, T. Yasuda^{ay}, Y.A. Yatsunenko^{aj}, Y. Yen^z, K. Yip^{bu},
 H.D. Yoo^{by}, S.W. Youn^{bb}, J. Yu^{bz}, A. Yurkewicz^{bt}, A. Zabi^p, A. Zatserklyaniy^{ba}, C. Zeitnitz^x,
 D. Zhang^{ay}, T. Zhao^{cd}, Z. Zhao^{bl}, B. Zhou^{bl}, J. Zhu^{bt}, M. Zielinski^{bs}, D. Zieminska^{bc},
 A. Zieminski^{bc}, V. Zutshi^{ba}, E.G. Zverev^{al}

^a Universidad de Buenos Aires, Buenos Aires, Argentina

^b LAFEX, Centro Brasileiro de Pesquisas Físicas, Rio de Janeiro, Brazil

^c Universidade do Estado do Rio de Janeiro, Rio de Janeiro, Brazil

^d Instituto de Física Teórica, Universidade Estadual Paulista, São Paulo, Brazil

^e University of Alberta, Edmonton, Alberta, Canada, Simon Fraser University, Burnaby, British Columbia, Canada, York University, Toronto, Ontario, Canada,
 and McGill University, Montreal, Quebec, Canada

^f Institute of High Energy Physics, Beijing, People's Republic of China

^g University of Science and Technology of China, Hefei, People's Republic of China

^h Universidad de los Andes, Bogotá, Colombia

ⁱ Center for Particle Physics, Charles University, Prague, Czech Republic

^j Czech Technical University, Prague, Czech Republic

^k Center for Particle Physics, Institute of Physics, Academy of Sciences of the Czech Republic, Prague, Czech Republic

^l Universidad San Francisco de Quito, Quito, Ecuador

^m Laboratoire de Physique Corpusculaire, IN2P3-CNRS, Université Blaise Pascal, Clermont-Ferrand, France

ⁿ Laboratoire de Physique Subatomique et de Cosmologie, IN2P3-CNRS, Université de Grenoble 1, Grenoble, France

^o CPPM, IN2P3-CNRS, Université de la Méditerranée, Marseille, France

^p IN2P3-CNRS, Laboratoire de l'Accélérateur Linéaire, Orsay, France

^q LPNHE, IN2P3-CNRS, Universités Paris VI and VII, Paris, France

^r DAPNIA/Service de Physique des Particules, CEA, Saclay, France

^s IReS, IN2P3-CNRS, Université Louis Pasteur, Strasbourg, France, and Université de Haute Alsace, Mulhouse, France

^t Institut de Physique Nucléaire de Lyon, IN2P3-CNRS, Université Claude Bernard, Villeurbanne, France

^u III. Physikalisches Institut A, RWTH Aachen, Aachen, Germany

^v Physikalisches Institut, Universität Bonn, Bonn, Germany

^w Physikalisches Institut, Universität Freiburg, Freiburg, Germany

^x Institut für Physik, Universität Mainz, Mainz, Germany

^y Ludwig-Maximilians-Universität München, München, Germany

^z Fachbereich Physik, University of Wuppertal, Wuppertal, Germany

^{aa} Panjab University, Chandigarh, India

^{ab} Delhi University, Delhi, India

^{ac} Tata Institute of Fundamental Research, Mumbai, India

^{ad} University College Dublin, Dublin, Ireland

^{ae} Korea Detector Laboratory, Korea University, Seoul, Republic of Korea

^{af} SungKyunKwan University, Suwon, Republic of Korea

^{ag} CINVESTAV, Mexico City, Mexico

^{ah} FOM-Institute NIKHEF and University of Amsterdam/NIKHEF, Amsterdam, The Netherlands

^{ai} Radboud University Nijmegen/NIKHEF, Nijmegen, The Netherlands

^{aj} Joint Institute for Nuclear Research, Dubna, Russia

^{ak} Institute for Theoretical and Experimental Physics, Moscow, Russia

^{al} Moscow State University, Moscow, Russia

^{am} Institute for High Energy Physics, Protvino, Russia

^{an} Petersburg Nuclear Physics Institute, St. Petersburg, Russia

^{ao} Lund University, Lund, Sweden, Royal Institute of Technology and Stockholm University, Stockholm, Sweden,
 and Uppsala University, Uppsala, Sweden

^{ap} Physik Institut der Universität Zürich, Zürich, Switzerland

^{aq} Lancaster University, Lancaster, United Kingdom

^{ar} Imperial College, London, United Kingdom

^{as} University of Manchester, Manchester, United Kingdom

^{at} University of Arizona, Tucson, AZ 85721, USA

^{au} Lawrence Berkeley National Laboratory and University of California, Berkeley, CA 94720, USA

^{av} California State University, Fresno, CA 93740, USA

^{aw} University of California, Riverside, CA 92521, USA

^{ax} Florida State University, Tallahassee, FL 32306, USA

- ^{ay} Fermi National Accelerator Laboratory, Batavia, IL 60510, USA
^{az} University of Illinois at Chicago, Chicago, IL 60607, USA
^{ba} Northern Illinois University, DeKalb, IL 60115, USA
^{bb} Northwestern University, Evanston, IL 60208, USA
^{bc} Indiana University, Bloomington, IN 47405, USA
^{bd} University of Notre Dame, Notre Dame, IN 46556, USA
^{be} Iowa State University, Ames, IA 50011, USA
^{bf} University of Kansas, Lawrence, KS 66045, USA
^{bg} Kansas State University, Manhattan, KS 66506, USA
^{bh} Louisiana Tech University, Ruston, LA 71272, USA
^{bi} University of Maryland, College Park, MD 20742, USA
^{bj} Boston University, Boston, MA 02215, USA
^{bk} Northeastern University, Boston, MA 02115, USA
^{bl} University of Michigan, Ann Arbor, MI 48109, USA
^{bm} Michigan State University, East Lansing, MI 48824, USA
^{bn} University of Mississippi, University, MS 38677, USA
^{bo} University of Nebraska, Lincoln, NE 68588, USA
^{bp} Princeton University, Princeton, NJ 08544, USA
^{bq} State University of New York, Buffalo, NY 14260, USA
^{br} Columbia University, New York, NY 10027, USA
^{bs} University of Rochester, Rochester, NY 14627, USA
^{bt} State University of New York, Stony Brook, NY 11794, USA
^{bu} Brookhaven National Laboratory, Upton, NY 11973, USA
^{bv} Langston University, Langston, OK 73050, USA
^{bw} University of Oklahoma, Norman, OK 73019, USA
^{bx} Oklahoma State University, Stillwater, OK 74078, USA
^{by} Brown University, Providence, RI 02912, USA
^{bz} University of Texas, Arlington, TX 76019, USA
^{ca} Southern Methodist University, Dallas, TX 75275, USA
^{cb} Rice University, Houston, TX 77005, USA
^{cc} University of Virginia, Charlottesville, VA 22901, USA
^{cd} University of Washington, Seattle, WA 98195, USA

Received 29 November 2005; accepted 13 April 2006

Available online 5 May 2006

Editor: M. Doser

Abstract

The cross section for the inclusive production of isolated photons has been measured in $p\bar{p}$ collisions at $\sqrt{s} = 1.96$ TeV with the DØ detector at the Fermilab Tevatron Collider. The photons span transverse momenta 23 to 300 GeV and have pseudorapidity $|\eta| < 0.9$. The cross section is compared with the results from two next-to-leading order perturbative QCD calculations. The theoretical predictions agree with the measurement within uncertainties.

© 2006 Elsevier B.V. All rights reserved.

PACS: 13.85.Qk; 12.38.Qk

Photons originating in the hard interaction between two partons are typically produced in hadron collisions via quark–gluon Compton scattering or quark–anti-quark annihilation [1–4]. Studies of these direct photons with large transverse momenta, p_T^γ , provide precision tests of perturbative QCD (pQCD) as well as information on the distribution of partons within protons, particularly the gluon. These data were, in the past, used in global fits of parton distributions functions (PDFs) and complement analyses of deep inelastic scattering,

Drell–Yan pair production, and jet production [5]. Photons from energetic π^0 and η mesons are the main background to direct photon production especially at small p_T^γ [6]. Since these mesons are produced inside jets, their contribution can be suppressed with respect to direct photons by requiring the photon be isolated from other particles. Isolated electrons from the electroweak production of W and Z bosons also contribute to the background at high p_T^γ . Previous measurements of photon production at hadron colliders successfully used these isolation techniques to extract the photon signal [7–13].

We present, in this Letter, a measurement of the cross section for the inclusive production of isolated photons with pseudorapidity $|\eta| < 0.9$ in $p\bar{p}$ collisions at $\sqrt{s} = 1.96$ TeV. (Pseudorapidity is defined as $\eta = -\ln \tan(\theta/2)$, where θ is the polar

* Corresponding author.

E-mail address: bandurin@fnal.gov (D.V. Bandurin).

¹ Visitor from Purdue University Calumet, Hammond, IN, USA.

² Visitor from Helsinki Institute of Physics, Helsinki, Finland.

angle with respect to the proton beam direction.) The data sample corresponds to an integrated luminosity $L = 326 \pm 21 \text{ pb}^{-1}$ [14] accumulated in 2002–2004 with the DØ detector [15] at the Fermilab Tevatron Collider. The primary tool for photon detection is the central part of a liquid-argon and uranium calorimeter covering $|\eta| < 1.1$. Two additional calorimeters, housed in separate cryostats, extend the coverage to $|\eta| < 4.2$ [16]. The electromagnetic section of the central calorimeter (EM) is segmented longitudinally into four layers (EM1–EM4) of 2, 2, 7, and 10 radiation lengths, respectively, and transversely into cells in η and azimuthal angle, $\Delta\eta \times \Delta\phi = 0.1 \times 0.1$ (0.05×0.05 in the EM3 layer at the electromagnetic shower maximum), yielding a good angular resolution for photons and electrons. The calorimeter surrounds a preshower detector and a tracking system which consists of silicon microstrip and scintillating fiber trackers (0.3 radiation lengths) located within a 2 T solenoidal magnet. The total amount of material between the interaction point and the first active layer of the calorimeter is equivalent to approximately 3.5–4.5 radiation lengths (increasing with $|\eta|$). The position and width of the Z boson mass peak were used to determine the EM calorimeter calibration factors and the EM energy resolution [17].

Photon candidates were formed from clusters of calorimeter cells within a cone of radius $\mathcal{R} = \sqrt{(\Delta\eta)^2 + (\Delta\phi)^2} = 0.4$; the energy was then recalculated from the inner core with $\mathcal{R} = 0.2$. Candidates were selected if there was significant energy in the EM calorimeter layers ($> 95\%$), and the probability to have a matched track was less than 0.1%, and they satisfied the isolation requirement $(E_{\text{total}}(0.4) - E_{\text{EM}}(0.2))/E_{\text{EM}}(0.2) < 0.10$, where $E_{\text{total}}(0.4)$ is the total energy in a cone with $\mathcal{R} = 0.4$ and $E_{\text{EM}}(0.2)$ is the EM energy within $\mathcal{R} = 0.2$. Photon candidates with energy measurements biased by calorimeter module boundaries and structures were removed from consideration; the geometric acceptance was $A = (84.2 \pm 1.5)\%$. Potential backgrounds from cosmic rays and leptonic W boson decays were suppressed by requiring the missing transverse energy, calculated from the vector sum of the transverse energies of calorimeter cells, to be less than $0.7p_T^\gamma$. The efficiency for the above requirements was estimated with direct photons generated by PYTHIA [18]. Events were processed with the GEANT detector simulation package and overlaid with detector noise and minimum bias interactions [15]. The efficiency (excluding acceptance) rose from $(82 \pm 5)\%$ at $p_T^\gamma \approx 24 \text{ GeV}$ to a plateau of $(92 \pm 3)\%$ at $p_T^\gamma > 110 \text{ GeV}$. We used $Z \rightarrow e^+e^-$ events [17], due to the similarity between electron- and photon-initiated showers, to verify the selection efficiencies estimated with the Monte Carlo simulation (MC). The photon sample was acquired with a three-level trigger system that relied on hardware signals from the calorimeter and fast, software-based, photon reconstruction. The trigger was $(71 \pm 9)\%$ efficient for photon candidates with $p_T^\gamma \approx 24 \text{ GeV}$, $(93 \pm 2)\%$ at $p_T^\gamma \approx 32 \text{ GeV}$ and greater than 98% for $p_T^\gamma > 40 \text{ GeV}$. Every event was required to have a vertex, reconstructed with at least three tracks, within 50 cm of the nominal center of the detector along the beam axis; the efficiency for this requirement ranged from $(90.0 \pm 0.3)\%$ to $(95.3 \pm 0.1)\%$ as a function of instantaneous luminosity.

Four variables were used to further suppress the background: the number of EM1 cells with energy greater than 400 MeV within $\mathcal{R} < 0.2$ and within $0.2 < \mathcal{R} < 0.4$, the scalar sum of the transverse momenta of tracks within $0.05 < \mathcal{R} < 0.4$, and the energy-weighted cluster width in the finely-segmented EM3 layer. Area-normalized distributions of these four variables in the signal and background MC, after application of the main selection criteria, are shown in Fig. 1 for the $44 < p_T^\gamma < 50 \text{ GeV}$ interval. These variables were input to an artificial neural network (NN), built with the JETNET package [19], to suppress background and to estimate the purity of the resulting photon sample. The NN was trained to discriminate between direct photons and background events. The background events, produced with QCD and electroweak processes in PYTHIA, were preselected with loose criteria to increase statistics and to exclude high-momentum bremsstrahlung photons produced from partons. The resulting NN output, O_{NN} , peaks at unity for signal events and at zero for background events. Events with $O_{\text{NN}} > 0.5$ were considered in this analysis, yielding a high photon selection efficiency of $(93.7 \pm 0.2)\%$ and good background rejection. The NN was tested in MC and data using electrons from Z boson decays; the resulting O_{NN} distributions are shown in Fig. 2. The systematic uncertainty on the signal efficiency for the O_{NN} requirement, estimated with electrons from the Z boson samples, is 2.4%.

The photon purity (\mathcal{P}), defined as the ratio of signal to signal plus background, was determined statistically for each p_T^γ bin. Distributions of the number of events as a function of O_{NN} are shown for data and MC in Fig. 3 for the $44 < p_T^\gamma < 50 \text{ GeV}$ interval. The MC signal and background events in this figure were weighted by the fractions that resulted from the fit of the normalized linear combination of the MC events to data. The fit was performed with the CERNLIB fitting package HMCMLL [20]. The data are well described by the sum of MC signal and background samples, especially for events with $O_{\text{NN}} > 0.5$. Photon purities are shown in Fig. 4 as a function of p_T^γ . The purity uncertainty is dominated by MC statistics at low p_T^γ and data statistics at high p_T^γ . Systematic uncertainties were estimated by using two alternate fitting functions and by varying the number of bins used in the HMCMLL fits. The PYTHIA fragmentation model was an additional source of systematic uncertainty. This uncertainty was estimated by varying the production rate of π^0 , η , K_S^0 , and ω mesons by $\pm 50\%$ [21] resulting in an uncertainty of 7.5% at $p_T^\gamma \approx 24 \text{ GeV}$, 2% at $p_T^\gamma \approx 50 \text{ GeV}$, and 1% for $p_T^\gamma > 70 \text{ GeV}$.

The isolated-photon cross section is measured using the following definition:

$$\frac{d^2\sigma}{dp_T d\eta} = \frac{NPU}{L\Delta p_T^\gamma \Delta\eta A\epsilon}, \quad (1)$$

where N is the number of photon candidates, ϵ is the combined efficiency for the selection criteria described above, and Δp_T^γ and $\Delta\eta$ are the bin sizes. The factor U corrects the cross section for the effects of the finite resolution of the calorimeter. This unsmearing was performed, as a function of p_T^γ , by iteratively fitting the convolution of an ansatz function with an energy resolution function. The uncertainty in this correction

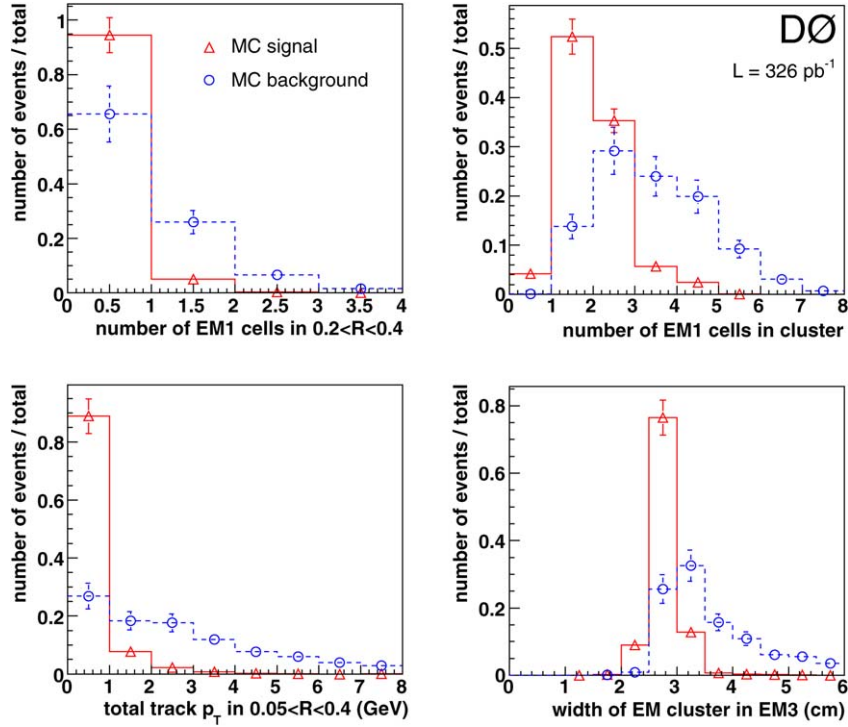


Fig. 1. Area-normalized distributions of the four input variables to the NN, described in text, for the $44 < p_T^\gamma < 50$ GeV interval in MC signal (Δ , solid line) and background (\circ , dashed line).

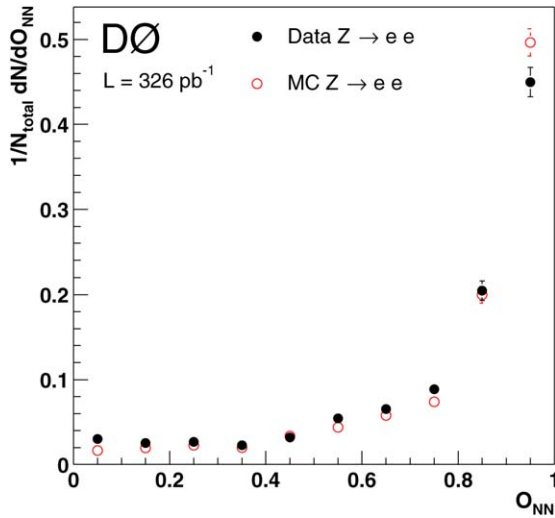


Fig. 2. Normalized distributions of NN output (O_{NN}) in $Z \rightarrow e^+e^-$ events for data (\bullet) and MC (\circ).

was estimated using two different ansatz functions and included the uncertainty in the energy resolution. An additional correction was applied to p_T^γ for the difference in the energy deposited in the material upstream of the calorimeter between electrons (used for the energy calibration) and photons. This correction to p_T^γ was approximately 1.9% at 20 GeV, 1.0% at 40 GeV, and less than 0.3% for $p_T^\gamma > 70$ GeV. The measured cross section, together with statistical and systematic uncertainties, is presented in Fig. 5 and Table 1. (The data points are plotted at the p_T value for which a smooth function describing the cross section is equal to the average cross section in the

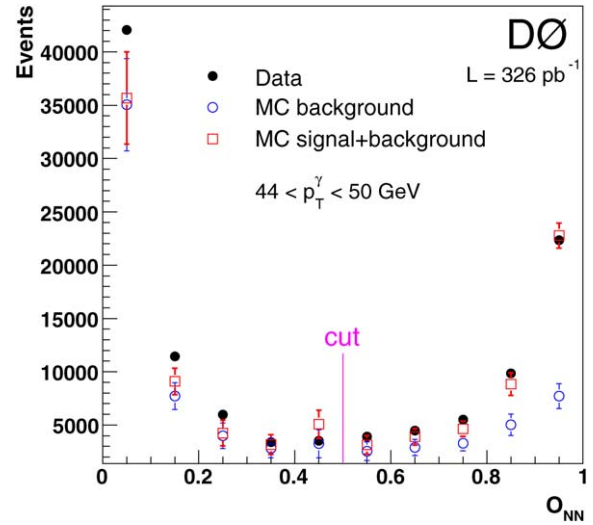


Fig. 3. Distribution of the number of events in data (\bullet) as a function of the NN output (O_{NN}) for $44 < p_T^\gamma < 50$ GeV. The contributions from MC background (\circ) and summed MC signal and background (\square) are also shown. The MC points were weighted according to the fitted purity (only statistical uncertainties are shown).

bin [22].) Sources of systematic uncertainty include luminosity (6.5%), event vertex determination (3.6%–5.0%), energy calibration (9.6%–5.5%), the fragmentation model (7.3%–1.0%), photon conversions (3%), and the photon purity fit uncertainty (shown in Fig. 4) as well as statistical uncertainties on the determination of geometrical acceptance (1.5%), trigger efficiency (11%–1%), selection efficiency (5.4%–3.8%) and unsmearing (1.5%). The uncertainty ranges above are quoted with the un-

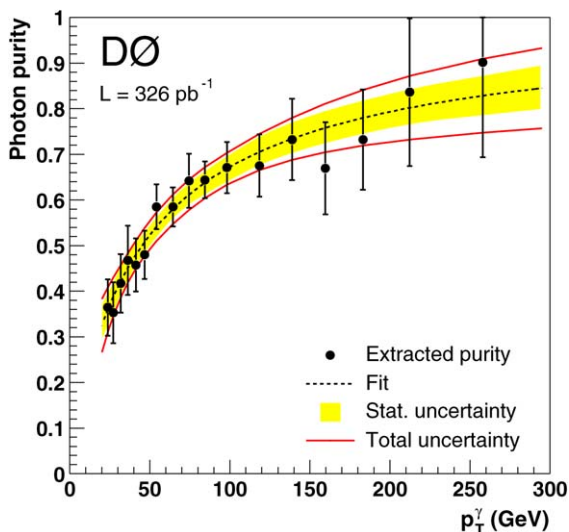


Fig. 4. Dependence of the photon purity on p_T^γ . The dashed line represents a fit to these points, the filled area corresponds to the statistical uncertainty band, and the solid lines to the total uncertainty band. The NN output in data was fit to the shapes of the MC signal and background samples.

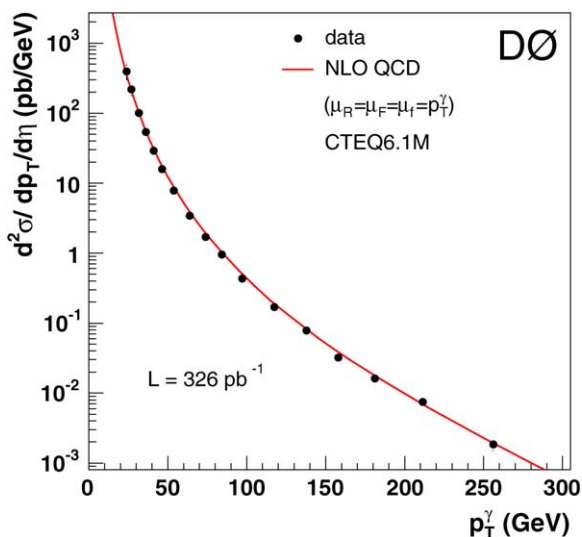


Fig. 5. The inclusive cross section for the production of isolated photons as a function of p_T^γ . The results from the NLO pQCD calculation with JETPHOX are shown as solid line.

certainty at low p_T^γ first and the uncertainty at high p_T^γ second. Most of these systematic uncertainties have large ($> 80\%$) bin-to-bin correlations in p_T^γ . Varying the choice of NN cut from 0.3 to 0.7 changed the measured cross section by less than 5%. The variation in the cross section was 4–6% for 50% changes in the isolation requirement.

Results from a next-to-leading order (NLO) pQCD calculation (JETPHOX [23,24]) are compared to our measured cross section in Fig. 5. These results were derived using the CTEQ6.1M [25] PDFs and the BFG [26] fragmentation functions (FFs). The renormalization, factorization, and fragmentation scales were chosen to be $\mu_R = \mu_F = \mu_f = p_T^\gamma$. Another NLO pQCD calculation [27], based on the small-cone approximation and utilizing different FFs [28], gave consistent results

Table 1

The measured differential cross section for the production of isolated photons, averaged over $|\eta| < 0.9$, in bins of p_T^γ . $\langle p_T^\gamma \rangle$ is the average p_T^γ within each bin. The columns $\delta\sigma_{\text{stat}}$ and $\delta\sigma_{\text{syst}}$ represent the statistical and systematic uncertainties respectively. (Five events with $p_T^\gamma > 300$ GeV, including one with $p_T^\gamma = 442$ GeV, were not considered in this analysis.)

p_T^γ (GeV)	$\langle p_T^\gamma \rangle$ (GeV)	$d^2\sigma/dp_T^\gamma d\eta$ (pb/GeV)	$\delta\sigma_{\text{stat}}$ (%)	$\delta\sigma_{\text{syst}}$ (%)
23–25	23.9	4.14×10^2	0.1	23
25–30	26.9	2.21×10^2	0.1	19
30–34	31.7	1.01×10^2	0.2	16
34–39	36.0	5.37×10^1	0.2	15
39–44	41.1	2.88×10^1	0.3	14
44–50	46.5	1.58×10^1	0.4	13
50–60	53.8	7.90×10^0	0.4	13
60–70	63.9	3.39×10^0	0.6	13
70–80	74.1	1.68×10^0	0.9	12
80–90	84.1	9.34×10^{-1}	1.3	12
90–110	97.2	4.38×10^{-1}	1.4	12
110–130	118	1.66×10^{-1}	2.3	12
130–150	138	7.61×10^{-2}	3.5	13
150–170	158	3.20×10^{-2}	5.6	13
170–200	181	1.59×10^{-2}	6.5	14
200–230	212	7.36×10^{-3}	9.8	14
230–300	256	1.81×10^{-3}	13	15

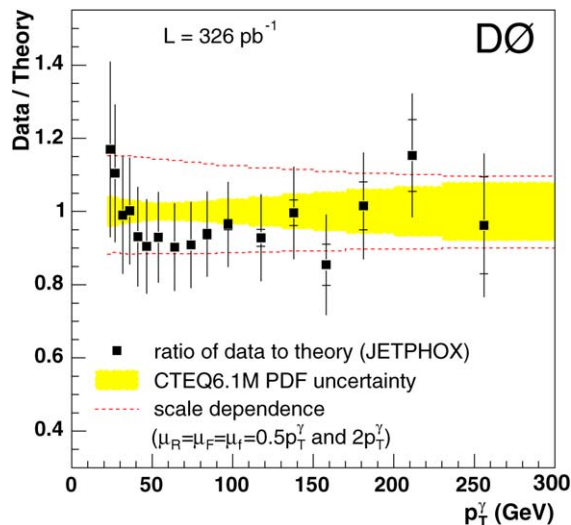


Fig. 6. The ratio of the measured cross section to the theoretical predictions from JETPHOX. The full vertical lines correspond to the overall uncertainty while the internal line indicates just the statistical uncertainty. Dashed lines represents the change in the cross section when varying the theoretical scales by factors of two. The shaded region indicates the uncertainty in the cross section estimated with CTEQ6.1 PDFs.

(within 4%). As shown in Fig. 6, the calculation agrees, within uncertainties, with the measured cross section. The scale dependence in the NLO pQCD theory, estimated by varying scales by factors of two, are displayed in Fig. 6 as dashed lines. The span of these results is comparable to the overall uncertainty in the cross section measurement. The filled area in Fig. 6 represents the uncertainty associated with the CTEQ6.1M PDFs. The central values of the predictions change by less than 7% when the PDFs are replaced by MRST2004 [29] or Alekhin2004 [30].

The calculation is also sensitive to the implementation of the isolation requirements including the hadronic fraction in the $\mathcal{R} = 0.2$ cone around the photon. The variation in the predicted cross section for 50% changes in the cut values for these criteria was found to be less than 3% [31]. The difference in shape between data and NLO pQCD at low p_T^γ in Fig. 6 is difficult to interpret due to the large correlated systematic uncertainties. NLO pQCD is consistent with data within uncertainties, however, results from calculations enhanced for soft-gluon contributions [6,32,33] also provide reasonable descriptions of the data.

In conclusion, we have measured the cross section for the production of isolated photons with $|\eta| < 0.9$ produced in $p\bar{p}$ collisions at $\sqrt{s} = 1.96$ TeV over a wide range in p_T^γ , $23 < p_T^\gamma < 300$ GeV. This extends previous measurements in this energy regime [9–13] to significantly higher values of p_T^γ . Results from NLO pQCD calculations agree with the measurement within uncertainties.

Acknowledgements

We thank W. Vogelsang, J.P. Guillet, E. Pilon, and M. Werlen for their assistance with theoretical calculations. We thank the staffs at Fermilab and collaborating institutions, and acknowledge support from the DOE and NSF (USA); CEA and CNRS/IN2P3 (France); FASI, Rosatom and RFBR (Russia); CAPES, CNPq, FAPERJ, FAPESP and FUNDUNESP (Brazil); DAE and DST (India); Colciencias (Colombia); CONACyT (Mexico); KRF and KOSEF (Korea); CONICET and UBACyT (Argentina); FOM (The Netherlands); PPARC (United Kingdom); MSMT (Czech Republic); CRC Program, CFI, NSERC and WestGrid Project (Canada); BMBF and DFG (Germany); SFI (Ireland); Research Corporation, Alexander von Humboldt Foundation, and the Marie Curie Program.

References

[1] J.F. Owens, Rev. Mod. Phys. 59 (1987) 465.

[2] P. Aurenche, et al., Phys. Lett. B 140 (1984) 87.
 [3] E.L. Berger, J.-w. Qiu, Phys. Lett. B 248 (1990) 371.
 [4] U. Baur, et al., hep-ph/0005226.
 [5] H.L. Lai, et al., Phys. Rev. D 55 (1997) 1280;
 A.D. Martin, et al., Eur. Phys. J. C 4 (1998) 463.
 [6] L. Apanasevich, et al., Phys. Rev. D 63 (2001) 014009.
 [7] C. Albajar, et al., UA1 Collaboration, Phys. Lett. B 209 (1988) 385.
 [8] J. Alitti, et al., UA2 Collaboration, Phys. Lett. B 288 (1992) 386.
 [9] F. Abe, et al., CDF Collaboration, Phys. Rev. Lett. 73 (1994) 2662.
 [10] B. Abbott, et al., DØ Collaboration, Phys. Rev. Lett. 84 (2000) 2786.
 [11] V.M. Abazov, et al., DØ Collaboration, Phys. Rev. Lett. 87 (2001) 251805.
 [12] D. Acosta, et al., CDF Collaboration, Phys. Rev. D 65 (2002) 112003.
 [13] D. Acosta, et al., CDF Collaboration, Phys. Rev. D 70 (2004) 074008.
 [14] T. Edwards, et al., DØ Collaboration, FERMILAB-TM-2278-E.
 [15] V.M. Abazov, et al., DØ Collaboration, Nucl. Instrum. Methods Phys. Res. A (2005) submitted for publication, physics/0507191.
 [16] S. Abachi, et al., DØ Collaboration, Nucl. Instrum. Methods A 338 (1994) 185.
 [17] V.M. Abazov, et al., DØ Collaboration, Phys. Rev. Lett. 95 (2005) 051802.
 [18] T. Sjöstrand, et al., Comput. Phys. Commun. 135 (2001) 238, PYTHIA v6.202.
 [19] C. Peterson, T. Rognvaldsson, L. Lönnblad, Comput. Phys. Commun. 81 (1994) 185.
 [20] R.J. Barlow, C. Beeston, Comput. Phys. Commun. 77 (1993) 219.
 [21] T. Sjöstrand, private communication;
 T. Binoth, et al., Eur. Phys. J. C 4 (2002) 7.
 [22] G.D. Lafferty, T.R. Wyatt, Nucl. Instrum. Methods A 355 (1995) 541.
 [23] T. Binoth, et al., Eur. Phys. J. C 16 (2000) 311.
 [24] S. Catani, et al., JHEP 0205 (2002) 028.
 [25] D. Stump, et al., JHEP 0310 (2003) 046.
 [26] L. Bourhis, M. Fontannaz, J.P. Guillet, Eur. Phys. J. C 2 (1998) 529.
 [27] L.E. Gordon, W. Vogelsang, Phys. Rev. D 48 (1993) 3136;
 L.E. Gordon, W. Vogelsang, Phys. Rev. D 50 (1994) 1901.
 [28] M. Gluck, E. Reya, A. Vogt, Phys. Rev. D 48 (1993) 116;
 M. Gluck, E. Reya, A. Vogt, Phys. Rev. D 51 (1995) 1427, Erratum.
 [29] A.D. Martin, R.G. Roberts, W.J. Stirling, R.S. Thorne, Phys. Lett. B 604 (2004) 61.
 [30] S. Alekhin, Phys. Rev. D 68 (2003) 014002.
 [31] W. Vogelsang, private communication.
 [32] E. Laenen, G. Oderda, G. Sterman, Phys. Lett. B 438 (1998) 173.
 [33] A. Lipatov, N. Zotov, hep-ph/0507243.